

TORSION OF A RECTANGULAR PRISMATIC BAR: SOLUTION USING A POWER FIT MODEL

Louis Angelo M. Danao* and Ryan M. Cabrera

Department of Mechanical Engineering
University of the Philippines-Diliman, Quezon City, Philippines
*email: louisdanao@up.edu.ph, louisdanao@gmail.com

ABSTRACT

The torsion problem of a rectangular prismatic bar is solved using the Saint-Venant's warping function method and analytic solutions to the twisting moment and the non-vanishing shear stresses are presented. Approximate solutions to the torsion problem are derived by curve-fitting the analytic solutions using a power fit model with the lengths of the rectangle sides as parameters. Errors observed did not exceed 0.6%. The study successfully presents a solution to the maximum non-vanishing shear stress at the narrow side of the rectangular section. Such a solution will be useful for the assessment of the critical points on a section that experiences combined bending and torsion loads.

Keywords: torsion, rectangular section, Saint-Venant, warping function, twisting moment, shear stress

1. INTRODUCTION

The general theory of torsion is very well established in literature and remains a classic in the field of solid mechanics and elasticity. Most often, problems concerning torsion, particularly that of prismatic bars, have great variety of engineering applications which range from analyzing stresses to designing of machine members and structures. Mostly, established solutions to torsion problems are for most cases given analytically. Only in some applications where difficulties in obtaining exact solutions may arise, numerical methods of solutions are sought. These difficulties are often a result of complexities in geometry or perhaps, the boundary conditions of the governing partial differential equation of the machine member or structure being analyzed. The most common of torsion problems encountered in engineering is that of circular-section bars. Only less familiar are those of triangular, elliptical, and rectangular sections. Among these

*Correspondence to: Department of Mechanical Engineering, University of the Philippines Diliman Quezon City, Philippines, email: louisdanao@up.edu.ph, louisdanao@gmail.com

geometries, analysis of rectangular-section bars is the most involved and is the main concern of this study. Although already well established in literature, for instance the classic text by Goodier and Timoshenko [1], it still remains a subject of interest for research.

Generally, in torsion problems, two methods of analyses or approaches are known: (i) the approach first introduced by Saint-Venant which uses displacement components and associated warping function; and (ii) the approach first introduced by Prandtl which uses the concept of membrane analogy and associated stress function. These approaches lead to solving torsion problems in the form of partial differential equations of either Laplace or Poisson type. In particular, Saint-Venant's approach yields Laplace's equation while Prandtl's approach yields Poisson's equation. In other words, torsion problems are generally boundary value problems (BVPs) which can be solved either analytically or numerically. Analytical methods of solutions are only practical when the cross-section of the prismatic bar being analyzed is regular, otherwise numerical solutions must be sought. In the case of rectangular sections, the method of Prandtl is common such as the one used in [1], because of its simplicity in boundary condition, i.e. of Dirichlet type. In contrast, the method of Saint-Venant is used in the text by Srinath [2], wherein the resulting boundary conditions are of Neumann type, which are nonhomogeneous. Nonetheless, one thing is common to both approaches and that is the method of solving the torsion BVP for rectangular sections is accomplished by Fourier series.

In a paper by Mindlin [3], the Saint-Venant's torsion problems are solved alternatively, by power series expansion, i.e. the Laplace equation is expressed as a double power series for which associated coefficients are obtained by simultaneous linear algebraic equations. For instance, in the case of rectangular sections, it is demonstrated in [3] that even if only four terms in the power series expansion are used, the obtained torsional rigidities have errors of less than 1.0 percent for square section to about 3.0 percent for a rectangle with ratio of 10:1 - which are already acceptable for practical purposes. Aside from the method of solution demonstrated in [3], torsion problems can also be solved by other means which are numerical such as the finite element method (FEM) and boundary element method (BEM). In particular, a p -Version FEM is demonstrated in the paper by Smith [4] while a dual-BEM is demonstrated in the paper by Chen et al. [5]. These numerical methods have been proven to be reliable means of solving torsion BVPs with very acceptable accuracy.

In torsion problems, results which are of main interest are expressions of the twisting moment and two non-vanishing shear stresses. In the case of rectangular sections, the expressions of the twisting moment and shear stresses are functions of rectangle ratio b/a , where a and b are half-lengths of the dimensions of narrow and wide sides of the rectangle, respectively. Of these two non-vanishing shear stresses, only the expression of the stress at the mid-wide sides of rectangular bars is commonly found in literature. In particular, [1] and [2] provide expression for this stress which are obtained from analytical solution, whereas Pytel and Singer [6] and Timoshenko [11] provide an approximate formula. This is because the stress at the mid-wide sides of rectangular bars is found to be the maximum torsional shear stress, which is therefore critical. Rarely provided in literature is the expression of the torsional shear stress at the mid-

narrow sides, practically because this stress is found to be lesser than the stress at mid-wide sides, and is therefore not critical. However, when dealing with problems involving rectangular sections under combined loading such as bending and torsion as well as two-plane bending with torsion, points which are critical may not be located at the points of maximum torsional shear stress. Other points which are potentially critical are at the mid-narrow sides of rectangular bars. Hence, with no solution to torsional shear stress but at the mid-wide sides, false conclusions may arise. This study is therefore primarily focused in finding the expression of the stress at the mid-narrow sides of rectangular bars.

In this paper, the development of torsion BVP for rectangular sections is done by Saint-Venant's approach. In other words, the resulting torsion problem is governed by Laplace equation, which has analytic solution in the form of infinite series. As a consequence, derived expressions of the twisting moment and torsional shear stresses at mid-narrow and mid-wide sides of rectangular bars are also in the form of infinite series. However, because these expressions are functions of rectangle ratio, then they can be related in a $2D$ – parametric plot. In particular, the x – data axis contains a range of values of rectangle ratio and the $y(x)$ – data axis as dimensionless twisting moment and shear stresses. Hence, instead of seeking for another method of solving the torsion BVP for rectangular sections such as in [3,4,5], this study is then motivated in finding approximate models of the twisting moment and shear stresses out of their analytic model counterparts. In other words, the approximate models are best fitted curves of the desired parameters as functions of rectangle ratio. In this study, the MATLAB[®] Curve Fitting Toolbox is used in selecting and obtaining the appropriate approximate models of the desired parameters. In this paper, the resulting models will be presented for two specific ranges of rectangle ratio, i.e. $[1 < (b/a) < 10]$ and $[10 < (b/a) < 100]$; wherein the models are continuous functions only for their corresponding range. In addition, comparison of models of the shear stress at the mid-wide sides of rectangular bars will be demonstrated. In particular, the resulting model obtained in this study and the one given in [6,11] will be compared, for each range of rectangle ratio, with the corresponding analytic model and relative errors will be presented.

2. TORSION PROBLEM FORMULATION: SAINT-VENANT'S APPROACH

Throughout this paper, the notation for the coordinate system used is indicial, i.e. (x_1, x_2, x_3) . The development of torsion BVP for any cross-section by means of Saint-Venant's approach, can be started by considering the stress tensor $[\sigma_{ij}]$; for $i, j = 1, 2, 3$. From Mase [7], this stress tensor is written as

$$[\sigma_{ij}] = \begin{bmatrix} \sigma_{11} & \sigma_{12} & \sigma_{13} \\ \sigma_{21} & \sigma_{22} & \sigma_{23} \\ \sigma_{31} & \sigma_{32} & \sigma_{33} \end{bmatrix} \quad (2.1)$$

where σ_{ij} for $i = j$ are known as the *normal stress components* while σ_{ij} for $i \neq j$ are known as *shear stress components*. In Figure 2.1, it should be observed that the first number of the indices denotes direction of axis normal to the plane where the stress component acts; while the second denotes direction of that stress. From conditions of equilibrium, the shear stress components are observed to be equal, i.e. $\sigma_{ij} = \sigma_{ji}$.

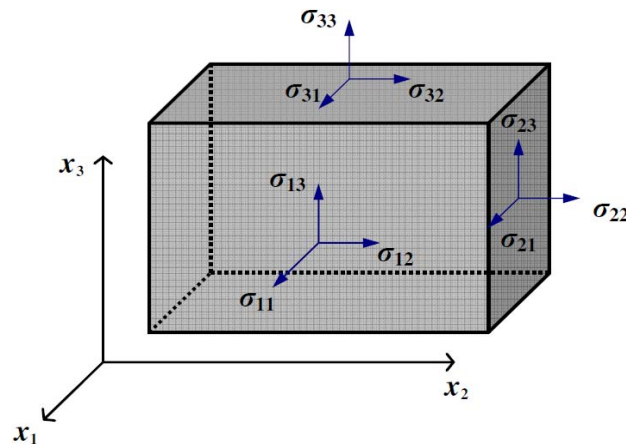


Fig. 2.1: Components of stress tensor at an arbitrary point of a continuum. The stresses are denoted in indicial notation.

The most important assumption in torsion BVP formulation is that the materials to be considered are *linearly elastic*, i.e. they obey Hooke's law. It is also assumed that the materials are *homogeneous* and *isotropic*, i.e. elastic properties are the same in all directions and in all parts of the body. From [7], the stresses are written as

$$\sigma_{ij} = 2G\varepsilon_{ij} + \frac{E\nu}{(1+\nu)(1-2\nu)}\varepsilon_{kk}\delta_{ij}; \text{ for } i, j, k = 1, 2, 3 \quad (2.2)$$

where the following material properties are: G as average shear modulus, E as Young's modulus of elasticity, and ν as Poisson's ratio. The terms ε_{ij} and ε_{kk} are the linearly elastic shear and normal strains, respectively. These strains are written as

$$\varepsilon_{ij} = \frac{1}{2} \left(\frac{\partial u_i}{\partial x_j} + \frac{\partial u_j}{\partial x_i} \right); \text{ for } i, j = 1, 2, 3 \quad (2.3)$$

Suppose a prismatic bar, of arbitrary length in the x_3 – direction, is subjected to twisting moment M coupled at both ends, then a rotation per unit length θ about the origin of (x_1, x_2) – plane is produced. Figure 2.2 shows an arbitrary cross-section of a general prismatic bar which serves as the torsion problem domain $\Omega = \Omega(x_1, x_2)$ bounded by Γ . The twisting moment couple causes a point $P(x_1, x_2)$ to be displaced to some point $P^*(x_1, x_2)$ in Ω . Figure 2.3 shows the displacement of point $P(x_1, x_2)$ to $P^*(x_1, x_2)$, in Ω of a rectangular section. From [1,2,3], the displacement components for any prismatic bar, are written as follows:

$$\begin{aligned} u_1(x_1, x_2, x_3) &= -\theta x_2 x_3 \\ u_2(x_1, x_2, x_3) &= \theta x_1 x_3 \\ u_3(x_1, x_2, x_3) &= \theta \psi(x_1, x_2) \end{aligned} \quad (2.4)$$

where $u_1(x_1, x_2, x_3)$ and $u_2(x_1, x_2, x_3)$ are called *in-plane displacements* in Ω , while $u_3(x_1, x_2, x_3)$ is the *axial* or *out-of-plane displacement* known as warping of cross-section and hence, $\psi = \psi(x_1, x_2)$ is called the associated *warping function*, which is not dependent on x_3 . This assumption follows Saint-Venant's hypothesis, i.e. the cross-sections are free to warp in the x_3 – direction but the warping is same for all cross-sections. But for circular sections, the (x_1, x_2) – plane remains plane and does not warp, i.e. there is no out-of-plane displacement component, and hence, only in-plane displacements are induced.

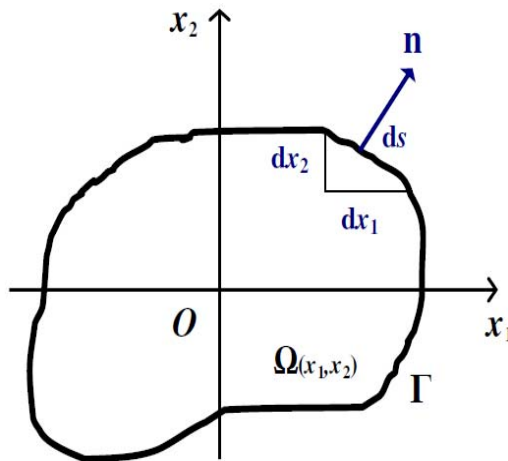


Fig. 2.2: Torsion problem domain for an arbitrary cross-section.

It should be noted from this point that the axis of rotation, or *center of twist*, is taken at the origin of the cross-section along the x_3 – direction. This assumption should not be overlooked, since it could affect the formulation of the torsion BVPs, especially if the cross-section has less than two axes of symmetry wherein the location of the center of twist can be unknown. This conventional torsion BVP formulation is common in [1,2,3]. In contrast, the non-conventional torsion BVP formulation is taken into account in the papers by Stronge and Zhang [8] and Li [9]; wherein instead of taking the origin of the (x_1, x_2) – coordinate system as the centroid of cross-section, as well the center of twist, an arbitrary reference coordinate system is considered. In particular, the coordinates of the center of twist are taken as offsets from the arbitrary coordinate system, i.e. $C(\eta_1, \eta_2)$; where η_1 and η_2 are the offset coordinates along x_1 – and x_2 – directions, respectively. This means that the centroid of section may not coincide with the center of twist.

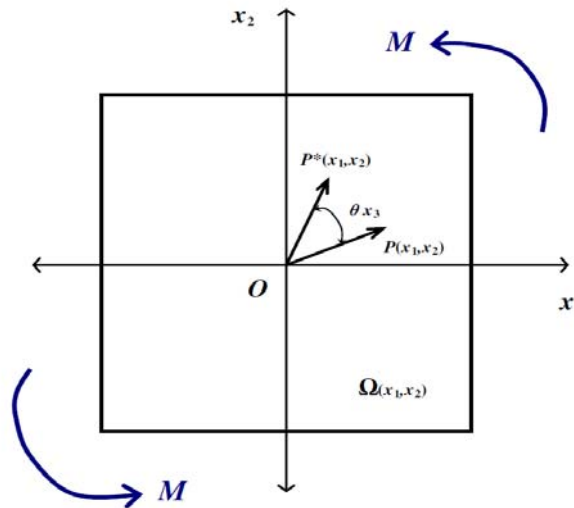


Fig. 2.3: Torsion problem domain for a rectangular cross-section subjected to a couple of twisting moment.

However, it is assumed in [8] that the center of twist $C(\eta_1, \eta_2)$ is coincident with the centroid, i.e. setting $\eta_1 = \eta_2 = 0$ is valid, if the cross-section has more than one axis of symmetry. Hence, for rectangular sections which have two axes of symmetry, it will be accepted, unless proven otherwise, that the center of twist is coincident with the centroid of section which can be taken at the origin of the (x_1, x_2) – coordinate system. It is also demonstrated in [9] that this should always be the case. In other words, the conventional torsion BVP formulation is safe to use and

will not affect the displacement components (2.4) written previously. Figure 2.4 shows the center of twist at the centroid of a prismatic bar of rectangular cross-section.

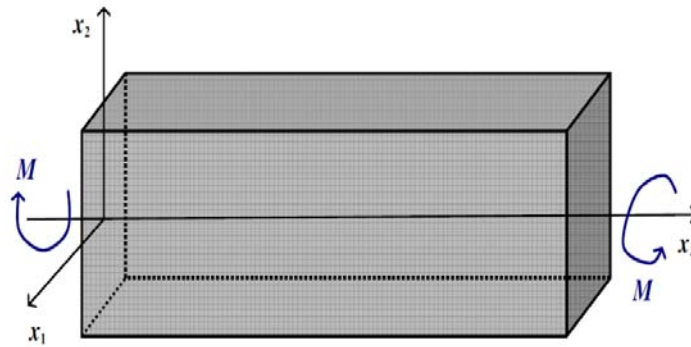


Fig. 2.4: Rectangular prismatic bar under coupled twisting moment at both ends.

Hence, by applying all previously stated assumptions, the torsion BVP formulation can now be established. By inserting (2.3) into (2.2) and noting (2.4), it is found that the non-vanishing shear stresses are

$$\sigma_{31} = G\theta \left(\frac{\partial \psi}{\partial x_1} - x_2 \right) \tag{2.5a}$$

$$\sigma_{32} = G\theta \left(\frac{\partial \psi}{\partial x_2} + x_1 \right) \tag{2.5b}$$

It should be noted that by using equations (2.2), (2.3), and (2.4), it can also be shown that the normal stresses σ_{ij} for $i = j$ and shear stress $\sigma_{12} = \sigma_{21}$ are zero. In other words, only shear stresses given by (2.5a) and (2.5b) are non-zero, which constitute a pure torsion problem.

By inserting the non-vanishing shear stresses into the equations of equilibrium given in [1,2], the Laplace equation for $\psi(x_1, x_2)$ is obtained as

$$\frac{\partial^2 \psi}{\partial x_1^2} + \frac{\partial^2 \psi}{\partial x_2^2} = \nabla^2 \psi(x_1, x_2) = 0; \text{ in } \Omega \tag{2.6}$$

where the boundary condition for (2.6) is given as

$$\left(\frac{\partial \psi}{\partial x_1} - x_2\right) \frac{dx_2}{ds} - \left(\frac{\partial \psi}{\partial x_2} + x_1\right) \frac{dx_1}{ds} = 0 ; \text{ on } \Gamma \quad (2.7)$$

Equations (2.6) and (2.7) constitute the torsion BVP for any cross-section of prismatic bars. For rectangular sections, the above BVP can be written as follows:

$$\frac{\partial^2 \psi}{\partial x_1^2} + \frac{\partial^2 \psi}{\partial x_2^2} = \nabla^2 \psi(x_1, x_2) = 0 ; \text{ in } [(-a < x_1 < a), (-b < x_2 < b)] \quad (2.8)$$

with boundary conditions

$$\frac{\partial \psi}{\partial x_1} = x_2 ; \text{ on } [x_1 = \pm a, (-b < x_2 < b)] \quad (2.9a)$$

$$\frac{\partial \psi}{\partial x_2} = -x_1 ; \text{ on } [(-a < x_1 < a), x_2 = \pm b] \quad (2.9b)$$

Figure 2.5 shows dimensions $2a$ and $2b$ of a rectangular section along the x_1 – and x_2 – directions, respectively.

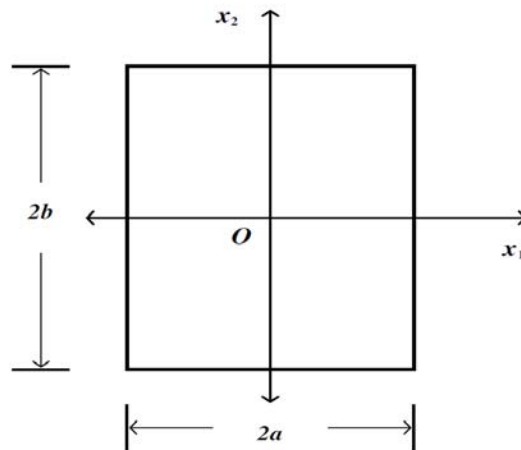


Fig. 2.5: Cross-section of rectangular prismatic bar showing dimensions.

It should be noted that Laplace equation (2.8) is apparently difficult to satisfy because of the Neumann type, non-homogeneous boundary conditions (2.9a) and (2.9b). However, it can still be solved by introducing a new appropriate function which is dimensionally homogeneous as the warping function.

3. SOLUTION OF SAINT-VENANT'S TORSION BVP FOR RECTANGULAR SECTIONS

The solution of the torsion BVP for rectangular sections can be accomplished by introducing a new function, say $\tilde{\psi} = \tilde{\psi}(x_1, x_2)$ that would satisfy Laplace equation (2.8), i.e. by transforming the problem in terms of $\psi(x_1, x_2)$ into a new one in terms of $\tilde{\psi}(x_1, x_2)$. The form of the solution associated with this transformation, as proposed in [2], is written as follows:

$$\psi(x_1, x_2) = x_1 x_2 - \tilde{\psi}(x_1, x_2) \quad (3.1)$$

such that (2.8) can be transformed into the form

$$\frac{\partial^2 \tilde{\psi}}{\partial x_1^2} + \frac{\partial^2 \tilde{\psi}}{\partial x_2^2} = \nabla^2 \tilde{\psi}(x_1, x_2) = 0; \text{ in } [(-a < x_1 < a), (-b < x_2 < b)] \quad (3.2)$$

Aside from satisfying Laplace equation (2.8), the transformation relationship (3.1) is necessary such that when it is applied to boundary condition (2.9a), a new boundary condition in terms of $\tilde{\psi}(x_1, x_2)$ is obtained. This transformed boundary condition is found to be *homogeneous*, i.e. zero on the boundary $[x_1 = \pm a, (-b < x_2 < b)]$, thus making the solution to (3.2) possible. The transformed boundary conditions corresponding to (2.9a) and (2.9b), respectively, are then written in terms of $\tilde{\psi}(x_1, x_2)$ as follows:

$$\frac{\partial \tilde{\psi}}{\partial x_1} = 0; \text{ on } [x_1 = \pm a, (-b < x_2 < b)] \quad (3.3a)$$

$$\frac{\partial \tilde{\psi}}{\partial x_2} = 2x_1; \text{ on } [(-a < x_1 < a), x_2 = \pm b] \quad (3.3b)$$

And by applying these transformed boundary conditions into (3.2), the appropriate form of the new function $\tilde{\psi}(x_1, x_2)$ is found to be

$$\tilde{\psi}(x_1, x_2) = \sum_{n=0}^{\infty} c_n \sin \kappa_n x_1 \sinh \kappa_n x_2 \quad (3.4)$$

where

$$\kappa_n = [(2n + 1)\pi / 2a]; \text{ for } n = 0, 1, 2, 3, \dots, \infty \quad (3.5)$$

And therefore the warping function (3.1) becomes

$$\psi(x_1, x_2) = x_1 x_2 - \sum_{n=0}^{\infty} c_n \sin \kappa_n x_1 \sinh \kappa_n x_2 \quad (3.6)$$

where, by following the method in the text by Zill [10], the Fourier coefficients c_n are written as

$$c_n = \frac{2}{\kappa_n \cosh \kappa_n b} \frac{\int_{-a}^a x_1 \sin \kappa_n x_1 dx_1}{\int_{-a}^a \sin^2 \kappa_n x_1 dx_1} \quad (3.7)$$

and by solving (3.7), c_n are obtained as follows:

$$c_n = \frac{32a^2}{\pi^3} \frac{(-1)^n}{(2n + 1)^3 \cosh \kappa_n b}; \text{ for } n = 0, 1, 2, 3, \dots, \infty \quad (3.8)$$

Therefore, the final form of warping function $\psi(x_1, x_2)$ is found be

$$\psi(x_1, x_2) = x_1 x_2 - \frac{32a^2}{\pi^3} \sum_{n=0}^{\infty} \frac{(-1)^n}{(2n + 1)^3} \frac{\sinh \kappa_n x_2}{\cosh \kappa_n b} \sin \kappa_n x_1 \quad (3.9)$$

where (3.9) is the solution to the torsion BVP for rectangular sections; and by inserting this function to expressions (2.5a) and (2.5b), the non-vanishing shear stresses are obtained as follows:

$$\sigma_{31} = -\frac{16G\theta a}{\pi^2} \sum_{n=0}^{\infty} \frac{(-1)^n}{(2n+1)^2} \frac{\sinh \kappa_n x_2}{\cosh \kappa_n b} \cos \kappa_n x_1 \quad (3.10a)$$

$$\sigma_{32} = 2G\theta x_1 - \frac{16G\theta a}{\pi^2} \sum_{n=0}^{\infty} \frac{(-1)^n}{(2n+1)^2} \frac{\cosh \kappa_n x_2}{\cosh \kappa_n b} \sin \kappa_n x_1 \quad (3.10b)$$

where σ_{31} and σ_{32} are the x_1 - and x_2 - components of the resultant shear stress σ in Ω , induced by the couple of twisting moment M .

The twisting moment is given as

$$M = \iint_{\Omega} (\sigma_{32} x_1 - \sigma_{31} x_2) d\Omega \quad (3.11)$$

and by inserting (3.10a) and (3.10b) into (3.11), M is obtained as

$$M = \frac{1}{3} G\theta (2a)^3 (2b) \left\{ 1 - \frac{192a}{\pi^5 b} \left[\tanh\left(\frac{\pi b}{2a}\right) + \sum_{n=1}^{\infty} \frac{\tanh \kappa_n b}{(2n+1)^5} \right] \right\} \quad (3.12)$$

where $\kappa_n = [(2n+1)\pi/2a]$, for $n = 1, 2, 3, \dots, \infty$; and it should be noted that the first term of the infinite series, i.e. $n = 0$, is evaluated judiciously. For rectangular sections, we are interested in the expressions for the non-vanishing shear stresses on Γ , particularly at the mid-narrow ($x_1 = 0, x_2 = \pm b$) and mid-wide ($x_1 = \pm a, x_2 = 0$) sides. It should be observed that for $b > a$, the non-vanishing shear stresses are $\sigma^* \equiv \sigma_{31}$ on ($x_1 = 0, x_2 = \pm b$) and $\sigma_{\max} \equiv \sigma_{32}$ on ($x_1 = \pm a, x_2 = 0$); where

$$\sigma^* = -\frac{16G\theta a}{\pi^2} \left[\tanh\left(\frac{\pi b}{2a}\right) + \sum_{n=1}^{\infty} \frac{(-1)^n}{(2n+1)^2} \tanh \kappa_n b \right] \quad (3.13a)$$

$$\sigma_{\max} = 2G\theta a - \frac{16G\theta a}{\pi^2} \left[\frac{1}{\cosh(\pi b/2a)} + \sum_{n=1}^{\infty} \frac{1}{(2n+1)^2 \cosh \kappa_n b} \right] \quad (3.13b)$$

It is important to emphasize that the magnitude of σ^* is lesser than σ_{\max} , i.e. $|\sigma^*| < |\sigma_{\max}|$, since the negative sign of (3.13a) only indicates direction. This is not difficult to prove because

the $2G\theta a$ term of (3.13b) governs the infinite series. The terms inside the brackets are observed to be functions only of the sides of the rectangular section. They can then be easily evaluated over the entire range of the rectangle ratio b/a . Figure 3.1 shows that at $b = a$, i.e. $(b/a) = 1$, the shear stress factors for both mid-narrow and mid-wide sides are equal thus $|\sigma^*| = |\sigma_{\max}|$.

In general, for rectangular bars in torsion, expressions for the twisting moment and the two non-vanishing shear stresses are functions of rectangle ratio b/a , with the assumption that $b > a$. Figure 3.1 shows the trend of the graph of dimensionless rigidity factor and shear stress factors as functions of b/a . It should be observed that these parameters are asymptotic for rectangle ratios practically greater than ten, i.e. $(b/a) \geq 10$. This asymptotic property of the graph of functions can be asserted from the fact that expressions for M , σ^* , and σ_{\max} have terms which are hyperbolic functions.

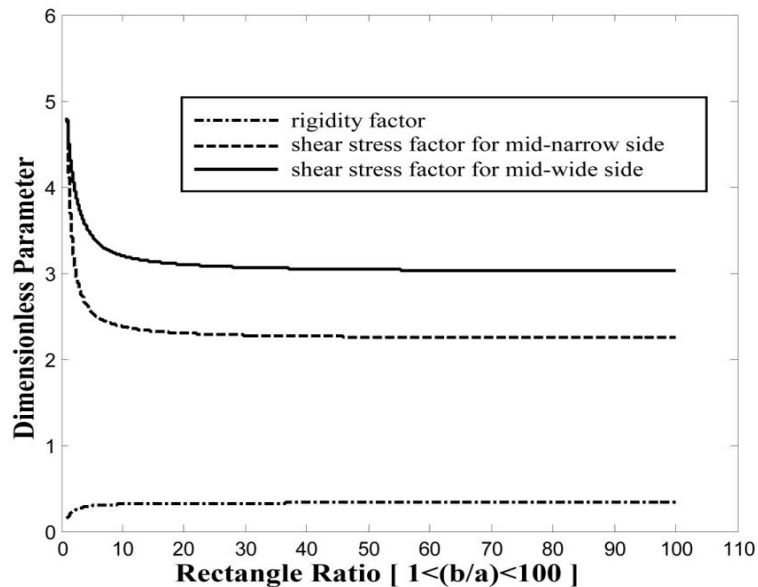


Fig. 3.1: Plot of rigidity factor and shear stress factors at mid-narrow and mid-wide sides as functions of rectangle ratio.

4. ANALYTIC MODELS

From the expressions of twisting moment M and torsional shear stresses σ^* and σ_{\max} derived in the previous section, analytic models of dimensionless parameters for rectangular bars will now be developed. These analytic models are continuous functions for any rectangle ratio, i.e. valid for $[1 < (b/a) < \infty]$.

4.1 Twisting Moment

For the twisting moment M , the corresponding dimensionless parameter is denoted as K , which can be called *rigidity factor*. Figure 4.1 shows the graph of this parameter for rectangle ratio range of $[1 < (b/a) < 100]$, whereas Table 4.1 tabulates the values of K for certain rectangle ratio within the range $[1 < (b/a) < 10]$. The twisting moment is given by (3.12), and is rewritten as

$$M = KG\theta(2a)^3(2b) = 16KG\theta a^3b; \text{ for } [1 < (b/a) < \infty] \quad (4.1)$$

where

$$K \equiv \frac{1}{3} \left\{ 1 - \frac{192}{\pi^5} \frac{a}{b} \left[\tanh \left(\frac{\pi b}{2a} \right) + \sum_{n=1}^{\infty} \frac{1}{(2n+1)^5} \tanh \left(\frac{(2n+1)\pi b}{2a} \right) \right] \right\}$$

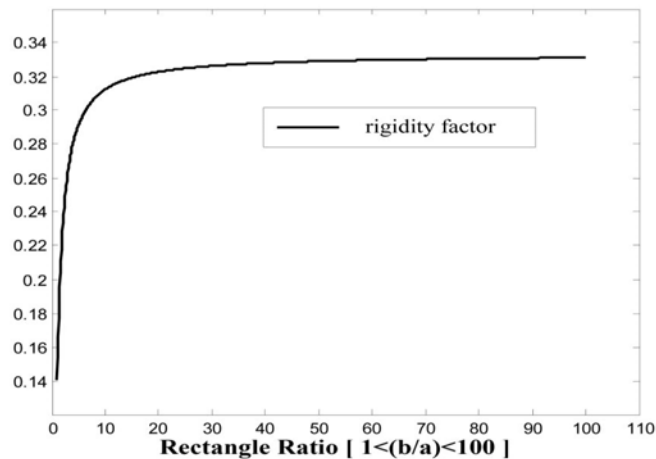


Fig. 4.1: Plot of rigidity factor as function of rectangle ratio.

Table 4.1: Rigidity factors for rectangular bars in torsion at different rectangle ratios.

b/a	1.0	1.2	1.5	2.0	2.5	3.0	4.0	5.0	10.0
K	0.1406	0.1661	0.1958	0.2287	0.2494	0.2633	0.2808	0.2913	0.3123

4.2 Shear Stresses

4.2.1. Mid-narrow Sides

The shear stress at the mid-narrow sides of a rectangular bar in torsion is given by (3.13a), and is rewritten as

$$\sigma^* = K_2^* \left[\frac{M}{(2a)^2(2b)} \right] = K_2^* \left[\frac{M}{8a^2b} \right]; \text{ for } [1 < (b/a) < \infty] \quad (4.2a)$$

where

$$K_1^* \equiv \frac{8}{\pi^2} \left[\tanh\left(\frac{\pi b}{2a}\right) + \sum_{n=1}^{\infty} \frac{(-1)^n}{(2n+1)^2} \tanh\left(\frac{(2n+1)\pi b}{2a}\right) \right]$$

$$K_2^* \equiv \frac{K_1^*}{K}$$

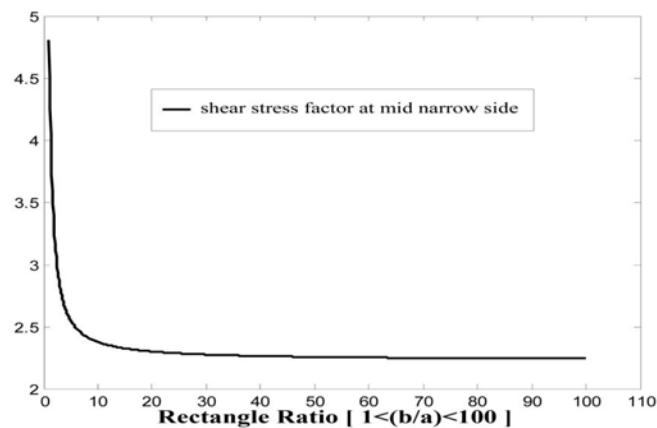


Fig. 4.2a: Plot of shear stress factor at mid-narrow sides as function of rectangle ratio.

Table 4.2a: Shear stress factors at mid-narrow sides of rectangular bars in torsion at different rectangle ratios.

b/a	1.0	1.2	1.5	2.0	2.5	3.0	4.0	5.0	10.0
K_1^*	0.6754	0.7060	0.7281	0.7395	0.7419	0.7424	0.7426	0.7426	0.7426
K_2^*	4.8046	4.2501	3.7195	3.2339	2.9753	2.8195	2.6443	2.5490	2.3775

4.2.2. Mid-wide Sides

The shear stress at the mid-wide sides of a rectangular bar in torsion is given by (3.13b), and is rewritten as

$$\sigma_{\max} = K_2 \left[\frac{M}{(2a)^2(2b)} \right] = K_2 \left[\frac{M}{8a^2b} \right]; \text{ for } [1 < (b/a) < \infty] \tag{4.2b}$$

where

$$K_1 \equiv 1 - \frac{8}{\pi^2} \left[\frac{1}{\cosh(\pi b / 2a)} + \sum_{n=1}^{\infty} \frac{1}{(2n+1)^2 \cosh[(2n+1)(\pi b / 2a)]} \right]$$

$$K_2 \equiv \frac{K_1}{K}$$

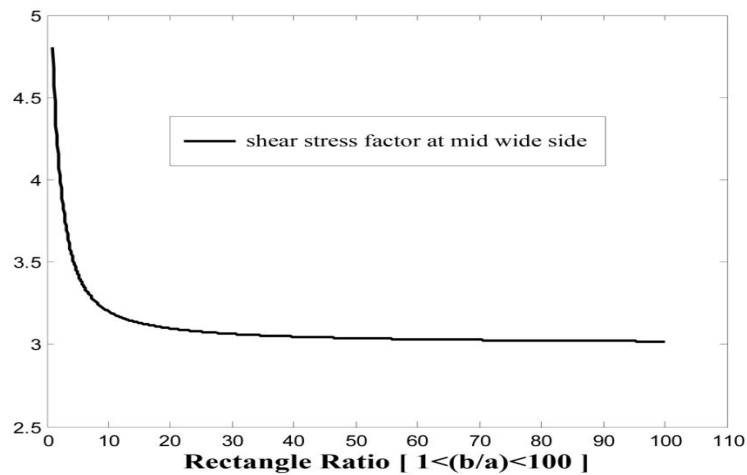


Fig. 4.2b: Plot of shear stress factor at mid-wide sides as function of rectangle ratio.

Table 4.2b: Shear stress factors at mid-wide sides of rectangular bars in torsion at different rectangle ratios.

b/a	1.0	1.2	1.5	2.0	2.5	3.0	4.0	5.0	10.0
K_1	0.6753	0.7588	0.8476	0.9301	0.9681	0.9854	0.9970	0.9994	1.0000
K_2	4.8039	4.5676	4.3296	4.0671	3.8821	3.7424	3.5503	3.4305	3.2018

5. APPROXIMATE MODELS

The approach of this study is to find models that will replace the complex expressions of the rigidity factor and the shear stress factors for the mid-narrow side and mid-wide side. A power fit model as well as polynomial models were tested and results show that the power fit model provides accuracy as well as practicality of use compared to the still complex and long polynomial fit. Other fits were tested but accuracy problems were encountered. The power fit models for the twisting moment and the two non-vanishing shear stresses $\tilde{\sigma}^*$ and $\tilde{\sigma}_{\max}$ all have \mathfrak{R}^2 -value better than 0.99.

5.1. Twisting Moment

The power fit model adopted for the twisting moment is as follows:

$$\tilde{M} = G\theta(2a)^3(2b) \left[\alpha \left(\frac{b}{a} \right)^\beta + \delta \right] = 16G\theta a^3 b \left[\alpha \left(\frac{b}{a} \right)^\beta + \delta \right] \quad (5.1)$$

where

α, β, δ are constants

Table 5.1: Power fit constants of approximate model for twisting moment of rectangular bars in torsion.

Rectangle Ratio	Power Fit Constants		
	α	β	δ
$[1 < (b/a) < 10]$	-0.2100	-0.9998	0.3333
$[10 < (b/a) < 100]$	-0.2099	-0.9996	0.3333

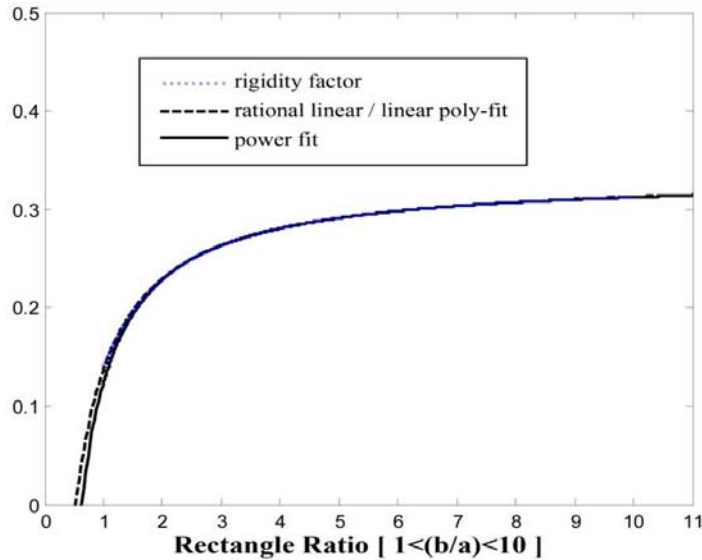


Fig. 5.1: Curve fit models of rigidity factor of rectangular bars in torsion; for rectangle ratio range of $[1 < (b/a) < 10]$.

5.2. Shear Stresses

5.2.1. Mid-Narrow Sides

The power fit model adopted for the shear stresses at the mid-narrow sides is as follows:

$$\tilde{\sigma}^* = \frac{M}{(2a)^2(2b)} \left[\alpha \left(\frac{b}{a} \right)^\beta + \delta \right] = \frac{M}{8a^2b} \left[\alpha \left(\frac{b}{a} \right)^\beta + \delta \right] \tag{5.2a}$$

where

α, β, δ are constants

Table 5.2a: Power fit constants of approximate model for shear stress at mid-narrow sides of rectangular bars in torsion.

Rectangle Ratio	Power Fit Constants		
	α	β	δ
$[1 < (b/a) < 10]$	2.539	-1.413	2.285
$[10 < (b/a) < 100]$	1.667	-1.051	2.229

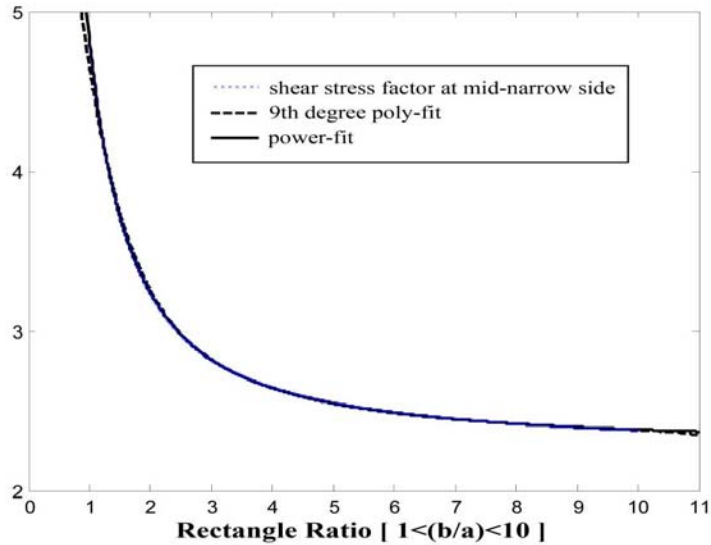


Fig. 5.2a: Curve fit models of shear stress factor at mid-narrow sides of rectangular bars in torsion; for rectangle ratio range of $[1 < (b/a) < 10]$.

5.2.2. Mid-wide Sides

The power fit model adopted for the shear stresses at the mid-wide sides is as follows:

$$\tilde{\sigma}_{\max} = \frac{M}{(2a)^2(2b)} \left[\alpha \left(\frac{b}{a} \right)^{\beta} + \delta \right] = \frac{M}{8a^2b} \left[\alpha \left(\frac{b}{a} \right)^{\beta} + \delta \right] \quad (5.2b)$$

where

α, β, δ are constants

Table 5.2b: Power fit constants of approximate model for shear stress at mid-wide sides of rectangular bars in torsion.

Rectangle Ratio	Power Fit Constants		
	α	β	δ
$[1 < (b/a) < 10]$	2.082	-0.677	2.745
$[10 < (b/a) < 100]$	2.245	-1.051	3.001

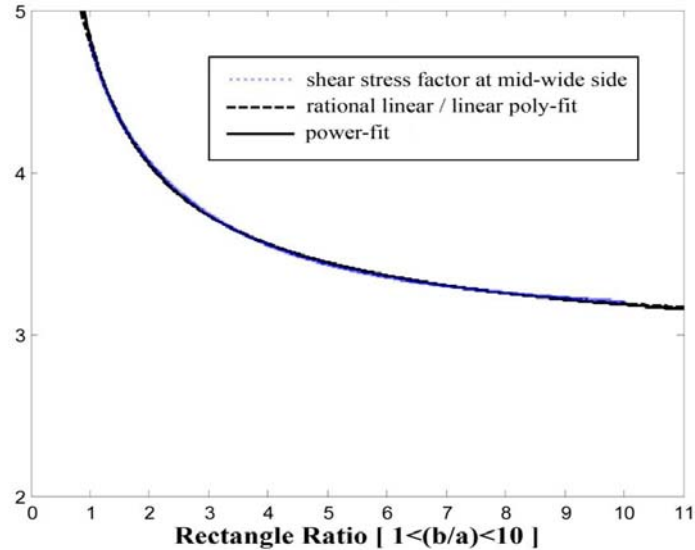


Fig. 5.2b: Curve fit models of shear stress factor at mid-wide sides of rectangular bars in torsion; for rectangle ratio range of $[1 < (b/a) < 10]$.

6. DISCUSSION OF RESULTS

The power fit model for the maximum shear stress factor is evaluated versus the analytic solution and it was observed that maximum errors did not exceed 0.6%. It is then compared to a well known published solution that resembles a power fit form. This well known solution is presented as early as 1930 when Timoshenko mentioned it in his book *Strength of Materials, Part I*. The solution, which we will call the *Timoshenko model*, takes the form [11]:

$$\tau_{\max} = \frac{M}{a^2 b} \left(3 + 1.8 \frac{a}{b} \right) \quad (6.1)$$

where τ_{\max} is the maximum shear stress at the mid-wide sides of the rectangular bar, as denoted by $\tilde{\sigma}_{\max}$ in this paper. Upon examination of this well known solution, one should notice that indeed it is a power fit model with the following constants: $\alpha = 1.8$, $\beta = -1$, and $\delta = 3$. The variables a and b are the lengths of the narrow and wide sides, respectively, and not half the lengths. When evaluated over the rectangle ratio range of 1 to 10, the maximum error that the solution gives is up to 4%. Beyond the rectangle ratio of 10, the *Timoshenko model* gives sufficiently accurate results. A comparison of the shear stress factors from the analytic solution,

Timoshenko model and the new solution, which we call the *present model*, over the rectangle ratio range of 1 to 10 and 10 to 100 is presented in Figs. 6.1 and 6.2, respectively.

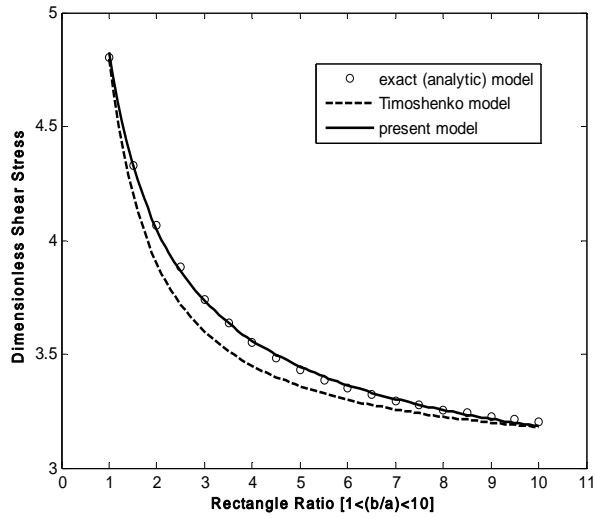


Fig. 6.1: Comparison of models of dimensionless shear stress at mid-wide sides of rectangular bars in torsion; for rectangle ratio range of $[1 < (b/a) < 10]$.

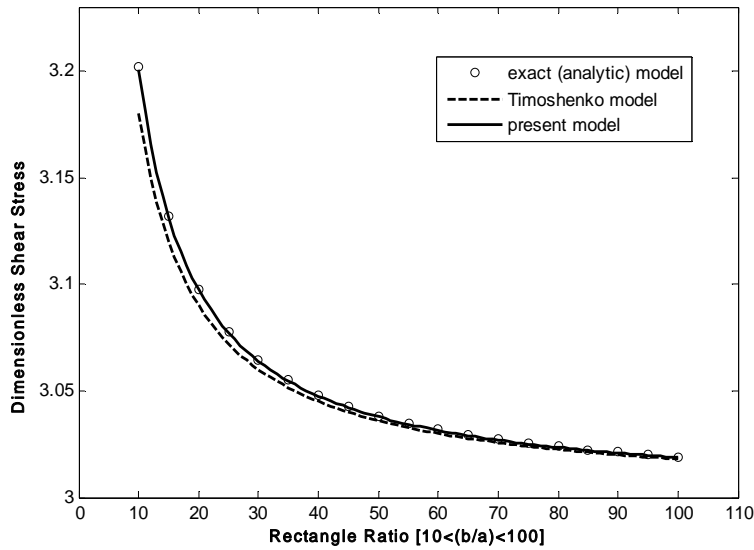


Fig.6.2: Comparison of models of dimensionless shear stress at mid-wide sides of rectangular bars in torsion; for rectangle ratio range of $[10 < (b/a) < 100]$.

7. CONCLUSION

One of the main problems that must be solved in the design of some load carrying elements subjected to torsion is to determine the shear stresses at critical points within a cross section and the angles of twist under a given torsional moment. The approximate model and the mathematical formulation presented in this paper allow for conducting uniform torsion analysis of rectangular solid cross sections. Easy and quickly calculable expressions of maximum shearing stresses for mid wide and mid narrow sides of the rectangular section have been derived. The shearing stresses are compared to analytical values. The results have shown that the obtained formulas give very accurate values. In conclusion, the model and the formulation presented in this paper are efficient and can help to solve the uniform torsion problem of a rectangular prismatic bar.

The value add of this study is the presentation of a solution to the unknown locally maximum torsional shear stress at the narrow side. With this available solution, more informed and educated assessment of the critical point in a particular section of a rectangular prismatic bar is possible. As mentioned previously, this is particularly important in combined loading problems where bending and torsion can induce maximum normal and/or shear stresses at a point other than the location of the maximum torsional shear stress.

ACKNOWLEDGEMENTS

Financial support from *Emerson Climate Technologies* and the *Engineering Research & Development for Technology (ERDT)* scholarship program is gratefully acknowledged. The ERDT scholarship program is initiated by the College of Engineering of the University of the Philippines (UPCOE), as the National Graduate School of Engineering (NGSE) of the country, for the purpose of developing and enhancing Filipino R & D through graduate education. This program is consistent with the Medium Term Development Plan (MTDP) and the National Science and Technology Plan (NSTP) of the country.

REFERENCES

1. Goodier, J. N. and Timoshenko, S. P., *Theory of Elasticity, 3rd ed.*, McGraw-Hill, 1970.
2. Srinath, L. S., *Advanced Mechanics of Solids, 2nd ed.*, Tata-McGraw-Hill, 2003.
3. Mindlin, R. D., "Solution of St. Venant's Torsion Problem by Power Series", *International Journal of Solid Structures*, Vol. 11, pp. 321-328, Pergamon Press, (1975).
4. Smith, J., "Highly Accurate Beam Torsion Solutions Using the p-Version Finite Element Method", *NASA Technical Paper 3608*, 1996.
5. Chen, J. T., Lin, S. R., and Chen, K. H., "Degenerate Scale for a Torsion Problem Using BEM", *Proceeding of the 3rd International Conference on BeTeQ*, Beijing China, 2002.
6. Pytel, A. and Singer, F.L., *Strength of Materials, 4th ed.*, HarperCollins Publishers, 1987.

7. Mase, G. E., *Schaum's Outline Series: Theory and Problems of Continuum Mechanics*, McGraw-Hill, Inc., 1970.
8. Stronge, W. J. and Zhang, T. G., "Warping of Prismatic Bars in Torsion", *International Journal of Solid Structures*, Vol. 30, pp. 601-606, Pergamon Press, (1993).
9. Li, S., "The Centre of Twist for a Prismatic Bar Under Free Torsion", *International Journal for Mechanical Engineering Education*, Vol. 33, pp. 226-232, (2003).
10. Zill, D. G., *Differential Equations with Boundary-Value Problems*, 2nd ed., PWS-KENT Publishing Company, 1989.
11. Timoshenko, S., *Strength of Materials, Part I: Elementary Theory and Problems*, D. Van Nostrand Company, 1st ed. 1930; 2nd ed., 1940; 3rd ed., 1955.